Propagation of ultrawideband short pulses of terahertz radiation through submillimeter-diameter circular waveguides

R. W. McGowan, G. Gallot, and D. Grischkowsky

School of Electrical and Computer Engineering and Center for Laser and Photonic Research, Oklahoma State University, Stillwater, Oklahoma 74078

Received June 11, 1999

We report experimental investigations in which quasi-optical methods were used to efficiently couple freely propagating, optoelectronically generated, subpicosecond pulses of terahertz (THz) radiation into submillimeter circular metal tubes (waveguides) and, consequently, to measure the transmitted pulses from these waveguides. We observe very dispersive low-loss propagation over the frequency band from 0.65 to 3.5 THz, with frequency-dependent group velocities v_g ranging from $c/4$ to c and phase velocities v_p from $4c$ to c, where $v_g v_p = c^2$. The linearly polarized incoming THz pulses couple significantly only into the TE_{11}, TM_{11}, and TE_{12} modes of the utilized 24- and 4-mm-long stainless-steel tubes, with inside diameters of 240 and 280 μm, respectively.

OCIS codes: 350.4010, 320.5390, 230.7370.

The advent of optoelectronic sources and receivers of subpicosecond pulses of terahertz (THz) electromagnetic radiation has generated much interest in the propagation properties of these pulses. For guided-wave propagation on coplanar transmission lines it has been shown that a picosecond electrical pulse cannot propagate more than approximately 1 cm, owing to Čherenkov-like radiation, which is equivalent (in the frequency domain) to the loss process of leaky waveguides.[1] In later studies in which silicon-on-insulator materials with a microstrip geometry[2] and thin-film microstrip lines[3] were used, the radiative loss, was eliminated, but the total observed loss owing to the dielectric and the metal was still approximately the same as for the coplanar transmission line. These problems disappear for the quasi-optical approach using freely propagating THz beams, in which subpicosecond THz pulses can propagate hundreds of centimeters without distortion.[4,5] For completeness we note that the reshaping of freely propagating THz pulses by passage through thin and thick metal slits has been experimentally and theoretically studied.[6,7] In previous microwave studies metal waveguides of up to 110 GHz were investigated.[8]

In this Letter we report what are believed to be the first experimental investigations using quasi-optical methods to efficiently couple freely propagating subpicosecond pulses of THz radiation into submillimeter circular metal tubes used as waveguides and consequently to measure the transmitted pulses from these waveguides. Within the passband of the waveguide, the measured power coupling into the waveguide was typically 40% of the incoming THz power. In agreement with theory,[9-11] at 1 THz the measured power absorption coefficient was $\alpha = 0.7\ \mathrm{cm}^{-1}$ for a 280-μm-diameter stainless-steel waveguide, compared (at 1 THz) with $\alpha = 14\ \mathrm{cm}^{-1}$ for coplanar transmission lines[1] and $\alpha = 18\ \mathrm{cm}^{-1}$ for thin-film microstrip lines.[3] At higher frequencies from 1 to 5 THz, the waveguide absorption of the dominant TE_{11} mode remains less than $0.7\ \mathrm{cm}^{-1}$, whereas the absorption of the thin-film microstrip line increases linearly with frequency f and that of the coplanar line increases as f^3. Although recent research has demonstrated techniques to reduce the radiation loss from coplanar lines,[12-14] the power absorption at higher frequencies remains well above $20\ \mathrm{cm}^{-1}$. Within our bandwidth we observe waveguide group velocities v_g ranging from $c/4$ to c, and phase velocities v_p from c to $4c$, where $(v_g v_p) = c^2$. This large group-velocity dispersion causes extensive pulse reshaping and broadening, resulting in a strongly negatively chirped pulse.

The experimental setup shown in Fig. 1(a) consists of an optoelectronic transmitter and receiver, along with THz beam-shaping and steering optics. In the standard THz–time-domain spectroscopy setup[4,5] the sample is placed at the THz beam waist between the two parabolic reflectors. For the waveguide experiment presented here a lens–waveguide–lens system is placed in this central position. For this system the hyperhemispherical silicon lenses[4,5] focus the THz beam to a frequency-independent $1/e$-waist diameter of 200 μm. The focused THz beam is coupled into and propagated through the circular metal waveguide and coupled out with the second silicon lens. The 24- and the 4-mm-long waveguides were cut from different 25-gauge stainless-steel hypodermic needles, the most accurate circular tubing that we could obtain, and had negligible ellipticity, with measured internal diameters of 240 and 280 μm, respectively.

We obtain the reference THz pulse by removing the waveguide and moving the two silicon lenses to near contact with a 300-μm-diameter aperture placed between them at their common focus. Figure 1(b) shows the reference THz pulse, and Fig. 1(c) shows that the useful amplitude spectrum extends from 0.1 to 4 THz. The transmitted signal from the 24-mm-long waveguide, Fig. 2(a), demonstrates the strong group-velocity dispersion of the waveguide, whereby the 1-ps input pulse has been stretched to ~70 ps,

0146-9592/99/201431-03$15.00/0

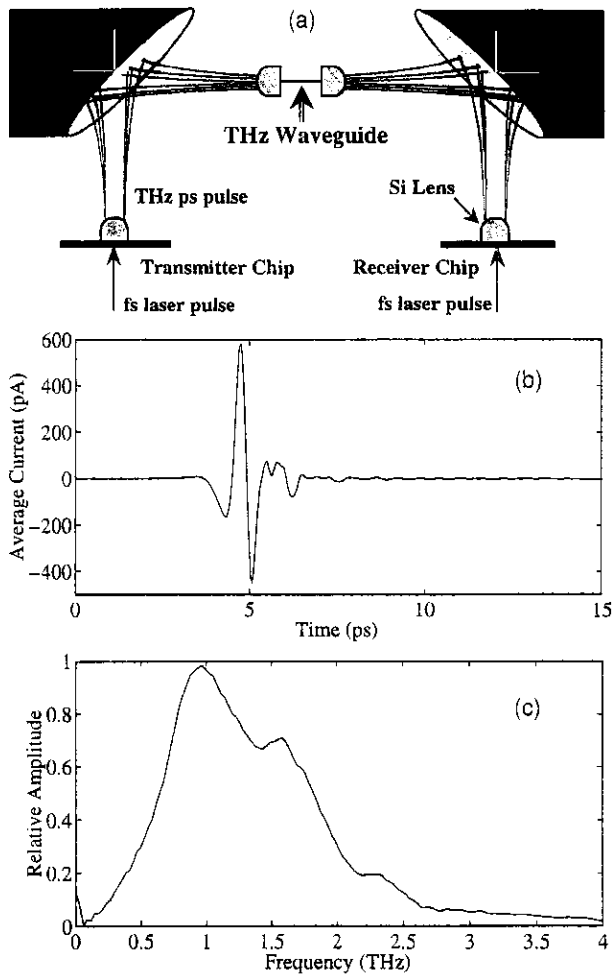

Fig. 1. (a) Schematic diagram of the optoelectronic THz–time-domain spectroscopy system, incorporating quasi-optical coupling into the investigated THz waveguide. (b) Measured reference THz pulse. (c) Relative amplitude spectrum of the reference pulse.

with the high frequencies arriving earlier in time, corresponding to negative chirp. The spectrum of this transmitted pulse, Fig. 2(b), shows a low-frequency cutoff at 0.76 THz compared with the calculation of 0.76 THz (TE_{11} mode), including the conductivity of the stainless-steel waveguide.

Compared with the 24-mm-long waveguide, the transmitted pulse from the 4-mm-long waveguide [Fig. 3(a)] displays much less cumulative dispersion; the pulse is spread over only 30 ps and shows fewer oscillations. Multimode behavior can be clearly observed in the late time oscillations, where several frequency components are interfering. The spectrum of this pulse, Fig. 3(b), shows the lowest-frequency cutoff at ~0.65 THz, which is also calculated (for stainless steel) to be 0.65 THz for the TE_{11} mode. The input spectrum from 0.1 to 4 THz, shown in Fig. 1(c), overlaps the cutoff frequencies of 30 modes of the 280-μm-diameter waveguide. However, the incoming linearly polarized THz pulse couples significantly into only three modes: the dominant TE_{11} mode with a cutoff frequency of 0.65 THz (77%), the TM_{11} with a cutoff at 1.31 THz (20%), and the weakly coupled TE_{12} with a cutoff at 1.81 THz (3%); the percent of the total coupled power in each mode is indicated in parentheses. Because of the larger attenuation of the TM_{11} mode compared with the TE_{11} mode, multimode interference is observed to be stronger in the shorter waveguide, since the TM_{11} mode has not yet been significantly attenuated. The different complex propagation vectors[9–11] of these three modes lead to a complicated data analysis in the spectral region, in which the power is propagating simultaneously in three modes. However, there is a spectral region in which the THz power is propagating only in the TE_{11} mode.

We evaluated the amplitude coupling coefficients of all the possible modes of the circular waveguide in the frequency range of the incoming THz pulse by performing a numerical overlap integral between the incoming field and the field of the individual mode over the waveguide cross section.[9,10] By use of the spectrum of the reference pulse, a theoretical calculation for the output spectrum from the 4-mm waveguide was performed [solid curve, Fig. 3(b)] that included the three coupled modes, their respective cutoff frequencies, and their frequency-dependent complex propagation vectors. Comparison of the amplitude spectrum of the reference pulse, Fig. 1(c), with that of the transmitted THz pulse through the 4-mm-long waveguide illustrates the excellent coupling of the freely propagating THz pulse into the waveguide. The calculated output pulse is given by the inverse Fourier transform of the calculated complex output amplitude spectrum $E_{out}(\omega, z)$ and compares favorably with the experiment as shown in Fig. 3(a).

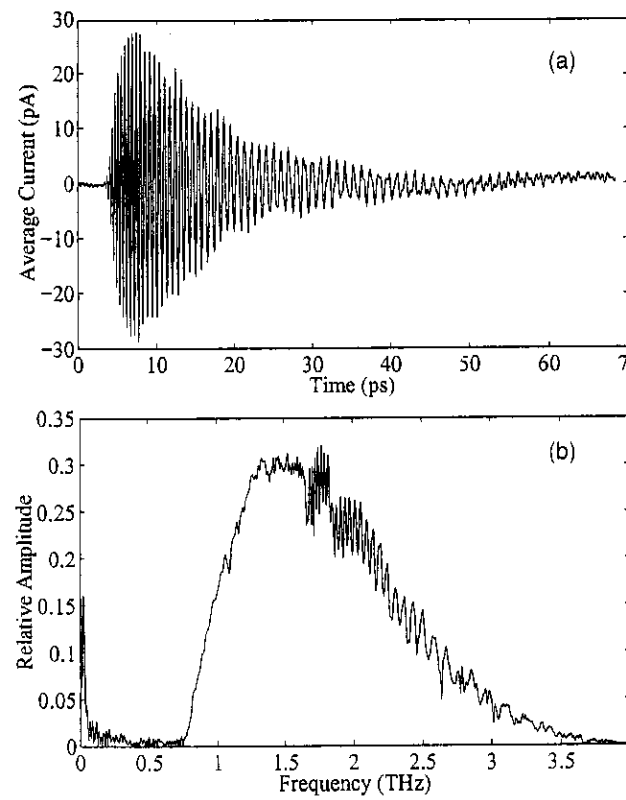

Fig. 2. (a) Measured THz pulse transmitted through a 24-mm-long 240-μm diameter stainless-steel waveguide. (b) Amplitude spectrum of the measured pulse (a).

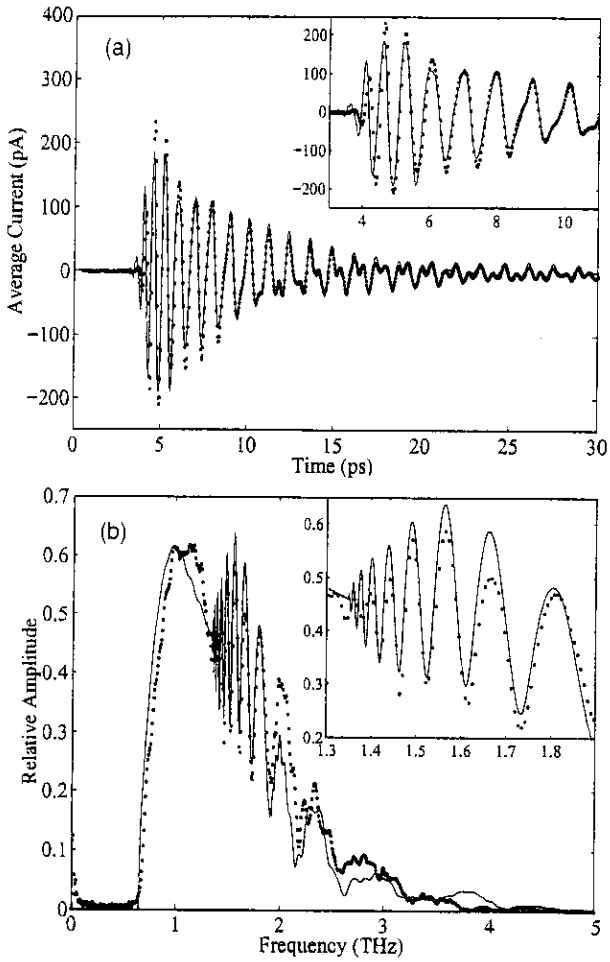

Fig. 3. (a) Measured THz pulse (dots) transmitted through a 4-mm-long 280-μm-diameter stainless-steel waveguide. (b) Amplitude spectrum (dots) of the measured transmitted pulse (a). The solid curves are the theoretical predictions, and the insets show an expanded scale.

Given the complex amplitude spectrum $E_{\text{in}}(\omega)$ of the reference pulse of Fig. 1, the detected complex amplitude spectrum is obtained from the relationship

$$E_{\text{out}}(\omega, z) = E_{\text{in}}(\omega, 0) \int_a \hat{e}_x \cdot \sum_n A_n \mathbf{E}_{tn} \exp[ik_n(\omega)z] \mathrm{d}a .$$

The integral is over the cross section of the waveguide, the summation is over all the modes of the waveguide, $\mathbf{E}_{tn}$ is the normalized transverse electric field of the nth mode, and A_n is the calculated amplitude coupling coefficient.[9,10] The complex propagation vectors $k_n(\omega)$ include both dispersion and absorption; z is the propagation distance. The output polarization direction $\hat{e}_x$ is parallel to the input polarization. The strong oscillations observed in the output spectrum are due to the interference of the $\hat{e}_x$-field components of the coupled modes propagating with different k vectors.

The observed extreme broadening of picosecond THz pulses owing to their waveguide propagation shows that for ultrawideband short-pulse time-domain applications such waveguides cannot be used. The broadening is caused by the extreme dispersion of the group velocity near the cutoff frequencies within the pulse spectrum.

Our final remarks pertain to promising applications of circular metal waveguides in frequency-domain investigations, in particular for surface-specific frequency-dependent absorption measurements. For an air-filled waveguide, the observed frequency-dependent absorption coefficient determines the frequency-dependent conductivity, which is difficult to obtain by other techniques. Long-path surface-specific measurements of molecular absorption to the metal waveguide walls is another area of promise. Such waveguides would also make excellent low-volume sample cells for high-pressure, long-path spectroscopic measurements of toxic or reactive gases and liquids.

We acknowledge careful readings of this manuscript by R. Alan Cheville and Steven Jamison. This work was partially supported by the National Science Foundation and the U.S. Army Research Office. D. R. Grischkowsky's e-mail address is danielg@thzsun.ecen.okstate.edu.

References

1. D. Grischkowsky, I. N. Duling III, J. C. Chen, and C.-C. Chi, Phys. Rev. Lett. **59,** 1663 (1987).
2. H. Roskos, M. C. Nuss, K. W. Goossen, D. W. Kisker, A. E. White, K. T. Short, D. C. Jacobson, and J. M. Poate, App. Phys. Lett. **58,** 2604 (1991).
3. J.-M. Heiliger, M. Nagel, H. G. Roskos, H. Kurz, F. Schnieder, W. Heinrich, R. Hey, and K. Ploog, Appl. Phys. Lett. **70,** 2233 (1997).
4. D. Grischkowsky, S. Keiding, M. van Exter, and Ch. Fattinger, J. Opt. Soc. Am. B **7,** 2006 (1990).
5. M. van Exter and D. Grischkowsky, IEEE Trans. Microwave Theory Tech. **38,** 1684 (1990).
6. A. Nahata and T. F. Heinz, IEEE J. Sel. Top. Quantum Electron. **2,** 701 (1996).
7. J. Bromage, S. Radic, G. P. Agrawal, C. R. Stroud, Jr., P. M. Fauchet, and R. Sobolewski, J. Opt. Soc. Am. B **15,** 1399 (1998).
8. C. E. Collins, J. W. Digby, R. D. Pollard, R. E. Miles, G. M. Parkhurst, J. M. Chamberlain, D. P. Steenson, N. J. Cronin, L. S. Karatzas, and J. W. Bowen, in *IEEE Microwave Theory and Technology Symposium Digest* (Institute of Electrical and Electronics Engineers, New York, 1997), Vol. 3, p. 1439.
9. J. C. Slater, Rev, Mod. Phys. **18,** 441 (1946).
10. N. Marcuvitz, *Waveguide Handbook* (Peregrinus, London, 1986).
11. S. Ramo, J. R. Whinnery, and T. van Duzer, *Fields and Waves in Communication Electronics*, 3rd ed. (Wiley, New York, 1994).
12. D. R. Dykaar, A. F. J. Levi, and M. Anzlowar, Appl. Phys. Lett. **57,** 1123 (1990).
13. H.-J. Cheng, J. F. Whitaker, T. M. Weller, and L. P. B. Katehi, IEEE Trans. Microwave Theory Tech. **42,** 2399 (1994).
14. R. W. McGowan and D. Grischkowsky, Appl. Phys. Lett. **71,** 2842 (1997).